Energy for Sustainable Development 38 (2017) 67–76

Contents lists available at ScienceDirect

Energy for Sustainable Development

Multifractal analysis of electricity demand as a tool for spatial forecasting

G. Salvó [a,b,*], M.N. Piacquadio [c]

[a] Edenor S.A., Ciudad Autónoma de Buenos Aires, Argentina
[b] Departamento de Electrotecnia, Facultad de Ingeniería, Universidad de Buenos Aires, Ciudad Autónoma de Buenos Aires, Argentina
[c] Secretaría de Investigación y Doctorado, Facultad de Ingeniería, Universidad de Buenos Aires, Ciudad Autónoma de Buenos Aires, Argentina

ARTICLE INFO

Article history:
Received 8 September 2016
Revised 26 February 2017
Accepted 28 February 2017
Available online xxxx

ABSTRACT

Electrical utilities need to plan their investments in substations and networks to meet future customer demand, by predicting the spatial load growth and its time trend. Several techniques are currently in use to do that, such as trending analysis or simulation methods. To study the electricity demand we used multifractal analysis. A fractal is an object whose irregularities are not smooth and have some self-similarity at different scales. If the fractal does not have strict self-similarity, we could break such fractality, if it really exists in the system, in a spectrum of sub fractals which have a self-similar structure, performing the so-called multifractal spectral analysis. Multifractal spectral analysis has been already applied to study the morphology and population growth of cities. Because electricity demand can be related to demographics of cities, it is possible to consider the hypothesis that multifractal spectral decomposition can be applied to analyze electricity demand. A variety of multifractal analyses were performed on real data from the customer demand of an electrical utility. The results show that the analyzed electricity demand is split into clear and interesting two-multifractal distribution with properties not found yet in the literature on the subject. This type of multifractal analysis could lead the way to improved spatial demand forecasting methods.

Introduction

According to Willis (2002), the methods currently in use by electric utilities to do spatial electric load forecasting can be divided into two main groups: non-analytic, mainly based on the judgment of the user (by using computer programs or not) with poor accuracy, and analytic. The analytic methods can be grouped into two categories: trending and simulation.

Trending methods use the past and present loads, fit a polynomial function to the historical data, and apply this function for extrapolating to the future, on an equipment-area basis, for example, feeders or substations. This method is most suited to large area forecasting, but it is not accurate for spatial forecasting in small areas with high spatial resolution (Willis, 2002).

On the contrary, simulation methods (Willis, 2002; Vieira Tahan and Pereyra Zamora, 2002; Sharma and Sreedhar, 2002) are useful in high spatial resolution and long-range forecasting. Simulation methods split the studied region into small areas, and then, by using some information about demographics, land-use, local geography, energy demand, etc., apply algorithms to forecast the demand in both aspects, spatial and temporal. These methods require more data than trending methods and they usually manage the two causes of electric load growth (change in the number of consumers and change in per capita consumption) separately.

Multifractal spectral analysis has been applied to study the morphology and population growth of cities (Thibault, 1995; Batty and Longley, 1994; Frankhauser, 1998; Tannier and Pumain, 2005; Kholladi, 2004; Czerkauer-Yamu and Frankhauser, 2010). The fractal approach in demography is at the same time a method of spatial analysis, a geometrical method to create model urban patterns, and an instrument for investigating the dynamics of cities. It reflects the hierarchical structure of cities and their irregularities and different scales, i.e., some kind of self-similarity, see below.

Thus, and since electricity demand is closely related to the demographics of cities, we proposed the following hypothesis: Can it be useful to apply multifractal spectral decomposition method to analyze electricity demand?

To answer this question and after a brief theoretical introduction to fractals and multifractal spectrum, we present the applied methodology

* Corresponding author at: Departamento de Electrotecnia, Facultad de Ingeniería, Universidad de Buenos Aires, Ciudad Autónoma de Buenos Aires, Argentina.
E-mail address: germansalvo@gmail.com (G. Salvó).

http://dx.doi.org/10.1016/j.esd.2017.02.005
0973-0826/

and the results of several multifractal decomposition calculations, and after some remarks about the obtained results, we proposed indices to analyze and characterize the demand.

Brief introduction to fractals

Fractal objects and fractal geometry generalize the "Euclidean dimension" and is better than Euclidean geometry for the spatial description of patterns from nature and from social organizations. The system properties described by fractal structures are heterogeneity, hierarchy and self-similarity (Tannier and Pumain, 2005).

In literature there is not a close definition to a fractal. A set "F" named as a fractal is characterized in terms of its properties (Falconer, 2003):

(i) F has a fine structure, i.e. detail at arbitrarily small scales.
(ii) F is too irregular to be described in traditional local and global geometric language (Euclidean).
(iii) Often F has some form of self-similarity (the same would be making a "zoom"), sometimes approximate or statistical.
(iv) Usually the "fractal dimension" F, defined in some way (by example, the box dimension d_B), is greater than their topological dimension (which would be $d_B = 1$ for a line or $d_B = 2$ for a surface).
(v) In most cases of interest F is defined in a simple way, and often recursively.

Fractals in nature are not only geometric. They also appear in several disciplines, as chemistry, astronomy, physics (including dielectric relaxation), social sciences, etc. (Rosen and Piacquadio, 2008; Piacquadio and Rosen, 2007; Jonscher, 1995; Jonscher, 1983; Piacquadio Losada, 2011). Fractals are in the very nature of a lot of natural phenomena.

A classic example of a geometric fractal is the "Cantor Set" which is obtained by eliminating, step by step, the central part of the segment, starting with unit length segment [0, 1] (Fig. 1). It is usual to suppose, going to infinite, that the "Cantor Set" becomes a set of points, and in this case their dimension has to be zero. But, it is wrong as we will see later.

Another fractal of interest, mainly in demography, is the "Sierpinski Carpet" (Fig. 2).

To calculate the box dimension "d_B" of the "Sierpinski Carpet", we can first consider a full square of unit side, and then we divide each side of the square into "n" equal parts. What we are doing is to cover the entire surface with small square boxes, also square all of them, in the form of a "regular grid", of side $L = 1/n$ (and which do not overlap each other). An amount of N boxes is required, where $N = n^2$ boxes (in the case similar of a cube $N = n^3$ boxes are required, all of them with length side $L = 1/n$). Note that the exponent "2" or "3", based on the power of $n = 1/L$, is responsible for the size dimension (Euclidean) of the object, "2" in the case of a square, "3" in the case of a cube.

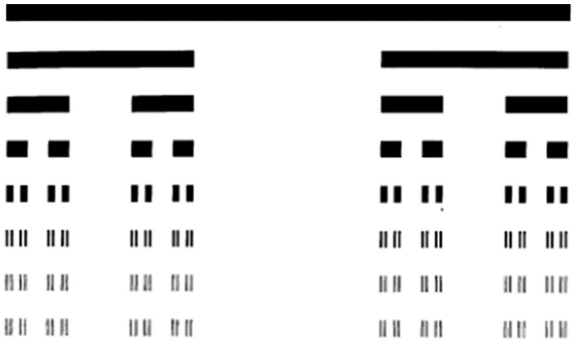

Fig. 1. "Cantor Set" (Mandelbrot, 1977).

These "2" or "3" exponents can be obtained with the following formula:

$$\frac{\text{Log N}}{\text{Log n}} = \frac{\text{Log N}}{\text{Log }(1/L)} = \frac{\text{Log N}(L)}{\text{Log }(1/L)}$$

for example,

$$\frac{\text{Log } n^2}{\text{Log }[(1/(1/n)]} = 2$$

In the "Sierpinski Carpet", i.e. a fractal in the R^2 plane, and after covering the entire surface with the "regular grid", we have to count the occupied boxes N(L). Then, the definition of box dimension, "d_B", is "Log N(L)/Log (1/L)", and the result is $d_B = \frac{\log 5}{\log 3} = 1.47$. For the "Cantor Set" the result is $d_B = \frac{\log 2}{\log 3} = 0.63$.

The word fractal comes from fracture or fraction, because it is not necessary for the expression "Log N(L)/log (1/L)" to be an integer, as shown above for the "Cantor Set" and for the "Sierpinski Carpet". "L" must be small, which means that, from a theoretical point of view, the expression "Log N(L)/log (1/L)" should go to the limit for $L \to 0$. But, in practice, this limit does not have empirical sense, and must be replaced by "L" as small as the experiment allows.

When a fractal object F has the same geometric structure in all its parts taken separately, when such a structure is identical to the one of the total object, and when it is independent of the scale, that is, the size of the parts tested, it is said that the fractal F is similar to their own parts, i.e., is "self-similar". Examples of strict self-similarity are found in the Cantor Set and the Sierpinski Carpet.

However, a "natural "or "real "fractal does not have that feature of strict self-similarity, then we could break such fractality, if exists in the reality of the system, in a spectrum of sub fractals which have a self-similar structure. Moreover, a real fractal contains some variable associated with each box, as weight, mass, population density or energy consumption of electrical energy. Such "weight" or "measure" (p_i), normalized to unity, is a distribution of probability on the fractal.

For each box B_i, with $i \in [1, N = n^2]$, we can define the "α-concentration" as "log–log" version of the density: $\alpha_i = \alpha(B_i) = \text{Log } p_i/\text{Log } L$.

We also define "f(α)" as the fractal dimension of the set of boxes with the same "α-concentration": $f(\alpha) = \text{Log } N_\alpha/\text{Log }(1/L)$, where N_α is the number of boxes with concentration "α". If we represent "f(α) vs. α", we obtain the multifractal spectrum of the fractal F. In Fig. 3 is shown the multifractal spectrum in a theoretical case in which it is possible to consider the limit conditions $L \to 0$, $N \to \infty$, and also $N_\alpha \to \infty$.

In accordance with Fig. 3 some general properties can be mentioned:

(i) $f''(\alpha) = d^2f/d\alpha^2 < 0$, which means that both branches of f(α) goes down.
(ii) f(α) is tangent to the bisector of the first quadrant $f(\alpha) = \alpha$ (as "$y = x$").
(iii) f(α) is tangent to the horizontal $f(\alpha) = d_B(F)$, which is the fractal dimension of the fractal set F.
(iv) The smallest values of α, α_{min} in particular, correspond to the "heavier" boxes, and the greatest values, in particular α_{max}, correspond to the "lighter" boxes, as can be easily demonstrated.

In practice, boxes with $N_\alpha = 1$ o $N_\alpha = 0$ are possible, then $\text{Log } N_\alpha = 0$ or ∞. To avoid this case, alpha interval [α_{min}, α_{max}] must be divided in a number of sub-intervals with length "Δα", and then make the counting of the α values within each interval. In this way we obtain reasonable N_α. The total number "N" of "alphas", i.e., the total number of occupied boxes, which determine the fractal dimension $d_B(F) = \text{Log N/Log }(1/L)$ is now exploded among several N_α. In one of the Δα intervals there is an "$\underline{\alpha}$" for which "f($\underline{\alpha}$)" is the maximum de

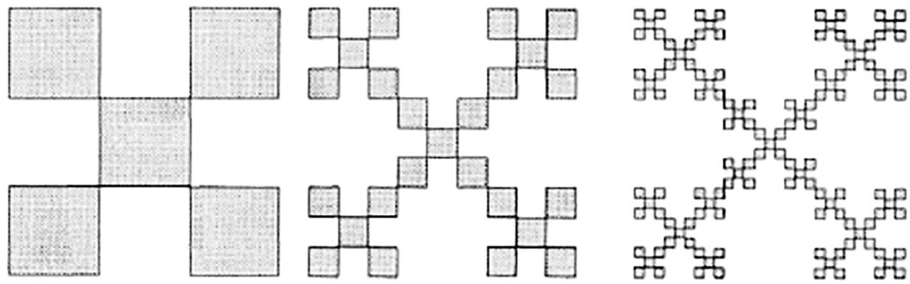

Fig. 2. "Sierpinski Carpet" (Frankhauser, 1998).

"f(α)", $f_{max} = \text{Log } N_{\underline{\alpha}}/\text{Log}(1/L)$. But $N_{\underline{\alpha}}$ is significantly smaller than N, then f_{max} cannot reach $d_B(F)$. Because of that, in an empirical situation, and if the nature of the analyzed phenomena can be represented by a multifractal spectrum, f(α) will be below the horizontal $d_B(F)$, and f(α) will go close to the bisector of the first quadrant $f(\alpha) = \alpha$ but will not be necessarily tangent to $f(\alpha) = \alpha$.

An empirical example of a multifractal is shown in Fig. 4.

Methodology

We worked with real data of the customer demand from an electrical utility. The data are in the form of maximum power density δ [MW/km^2] of one 2009 semester, placed geographically in coordinates (x,y), and defined in "boxes" of 500 m × 500 m, in a regular grid of 208 × 208 boxes = 43,264 boxes, many of them without demand, since there were no users in these areas, e.g. parks. The sample data available for the calculation comprised 6913 points.

If customer demand raw data were plotted in a city plan view, they show some areas with higher demand, and other with lower demand (Fig. 5). Data can be also grouped according to the MW/km^2, and/or according to the land use, for example rural or urban, but in this way they do not show any internal structure, as the structure we have found and that is presented below.

The "weight" or "measure"(p_i) of each box is the δ[MW/km^2], but normalized to unity divided by the total sum of "δ" from all boxes (one multifractal spectral analysis considers only those cases of positive measure and requires transforming the distribution of measures in a probability distribution), being the total sum as "T" of the entire grid. According to the definitions above, L = 1/208 is normalized for the unit side of the regular grid covering the study area. Then the "α-concentration" were calculated as "log–log" version of the density $\alpha_i = \alpha(B_i) = \text{Log } p_i/\text{Log } L$, and then these α_i have to be in order from lower to higher values, with "i" from 1 to 6913. As a result we obtained the lower value of α, $\alpha_1 = 1.02451$ and the higher, $\alpha_{6913} = 4.37516$.

After that we analyzed the obtained values of "α", because it is necessary to identify the representative values of fractal structure of the experiment, in the case of this fractality really exists (not all phenomena of nature can show fractal distributions).

At this point, we should clarify the concept of "Scattering of a Multifractal": In a "perfect", i.e., "mathematical" fractal object, each element is infinitely close to an infinite number of other elements fractal. However, in an experimental context, with empirical data from a real system, some elements may be far from the core (cluster) elements, where the studied fractal object is presumably concentrated. These boxes, correspond to ones not closer to others, but scattered. This phenomena is called "Scattering" and applied to the lighter boxes, found in the right zone of alphas, and that is the reason why it is named "Scattering at the right" (a pure, mathematical fractal does not have scattering, because it does not have isolated points). In the available data we found that between $\alpha_{6881} = 3.19445$ and $\alpha_{6913} = 4.37516$ there were only 32 data points, which means that these points do not belong to the system, or in multifractal language they are not in the fractal. They are the "Scattering at the right" and have to be removed from the analysis.

Looking into the 32 data points at the left zone of alphas, we did not find a similar "Scattering at the left". Then the results shown below are from the α_1 to α_{6881} range of values.

Results

Multifractal spectrum f(α)

The maximum theoretical dimension of the fractal is $d_B(F) = \text{Log N}/\text{Log }(1/L)$, in this case $d_B(F) = \text{Log } 6881/\text{Log }(208) = 1.6555$. For the empirical fractal the maximum value of f(α), f_{max}, will actually be significantly lower (for a square the dimension is "2").

The "alpha" range [$\alpha_{min} = \alpha_1 = 1.02451$; $\alpha_{max} = \alpha_{6881} = 3.19445$] has to be divided into a number of Δα intervals, for making the counting of α values inside each interval.

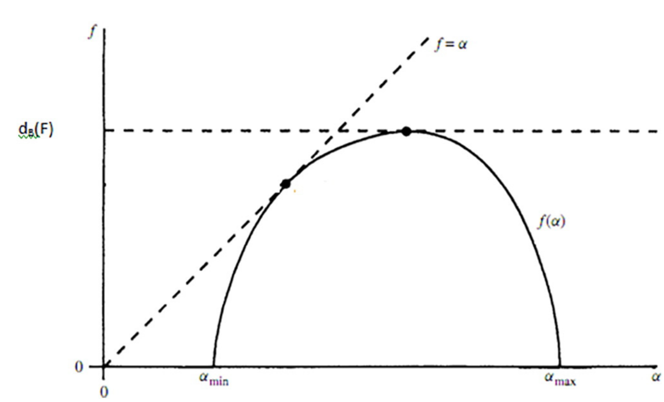

Fig. 3. Theoretical multifractal spectrum.
An adaptation from Falconer, (2003).

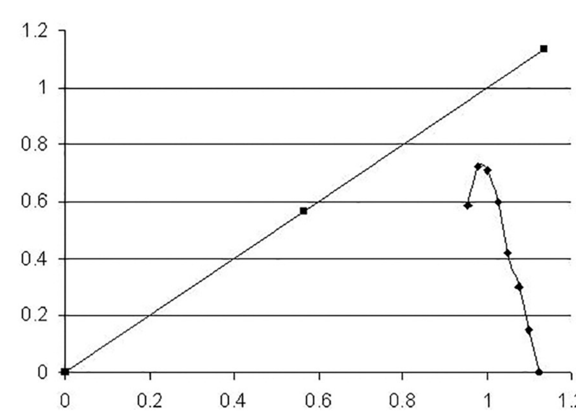

Fig. 4. Empirical example of multifractal spectrum.
Rosen and Piacquadio (2008).

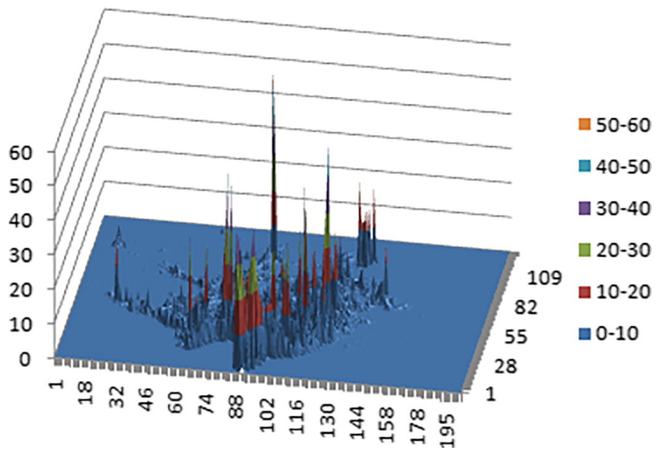

Fig. 5. Customer demand raw data plotted in a city plan view (Vertical axis: customer demand in arbitrary units; Horizontal axes: the boxes defined above).

Since the calculations were performed on finite samples, obtained empirically, it has been necessary to apply the criteria for the treatment of the data established in (Rosen and Piacquadio, 2008), i.e., to obtain a smooth curve $(\alpha, f(\alpha))$ and to "avoid" αs with no corresponding value of $f(\alpha)$. The number of $\Delta\alpha$ intervals has to be slightly smaller than that of the 4th root of the maximum number of boxes, in this case $(43264)^{1/4} \cong 14$ intervals.

Moreover, to obtain a value of f_{max} closer to $d_B(F)$, which means improving the quantitative aspects of $f(\alpha)$, a low number of intervals has to be chosen. To improve the qualitative aspects of $f(\alpha)$ it is necessary to choose a large number of intervals. After several calculations we decided to work with 11 and 9 intervals.

Results for 11 intervals $\Delta\alpha$

In Fig. 6 we present the multifractal spectrum obtained for 11 intervals, showing $(\mathrm{Ln}\ N_\alpha)$ instead of $(\mathrm{Log}\ N_\alpha/\mathrm{Log}\ L)$, without scaling factors, to give a qualitative image. The curve obtained seems to be the combination of two multifractals which is, at least, a finding for this field of knowledge.

As a confirmation for the election of 11 intervals, it can be said that 6881 points divided by 11 intervals, give about 625 per interval. Then, we can say that the unit for counting alphas could be 100, and for the first and last intervals, the numbers of 50 and 55 sound reasonable. Another selection of number of intervals have implied numbers of 10, 7 or even 1 alphas, which are unacceptable because they do not represent the phenomena properly.

A further calibration

By comparison between the left part of the points from Fig. 6 with Fig. 3, it must be made an additional analysis looking for a possible "Scattering at the left". Making a detailed analysis for the second decimal, we concluded that the seven first values of α can be discarded because their variation is more disordered than the variation for the rest of 43 elements of the first interval.

Despite discarding these elements, we have continued working with a precision of 99.9% of the total data, which is very acceptable in this empirical context. The results are shown in Fig. 7, where the only modified values are the ones in the first row, going from (Ln 50) to (Ln 43). The seven discarded boxes are abnormally heavy, and correspond to very high demanding consumers, that have to be out of the systematic analysis. Here it can be said that by doing a multifractal spectral analysis, it is possible to adjust the data universe to only the representative customer universe.

Characteristics of the multifractal spectrum

Two spectra were shown in Fig. 7, both with $f''(\alpha) = d^2f/d\alpha^2 < 0$. In Fig. 8, the two spectra are shown split.

The left spectrum, with α in the [1,2] interval, correspond with the boxes shown in red in Fig. 9. The right spectrum, with α in the [2,3] interval, correspond with the boxes shown in green in Fig. 9. We are going to name them as "Red spectrum" and "Green spectrum", and their correspondent fractals as "Red fractal" and "Green fractal".

It has to be noticed that the "Red spectrum" corresponds to a central region, or to a connected core, meanwhile the "Green fractal" corresponds to a peripheral zone, which surrounds or encircles the central red zone. Between the core and peripheral zones there exists a common frontier, pointed in Fig. 9 by the arrow, which will be later explained as the "Scattering of the red", with α slightly greater than 2.

Results for 9 intervals $\Delta\alpha$

In Fig. 8, and for 11 intervals, there were 5 intervals $\Delta\alpha$, i.e., 5 points $(\alpha, f(\alpha))$ for the red fractal, 5 for the green fractal, and 1 for the intermediate frontier. But, for 9 intervals (Fig. 10) there are 4 points for the red, 4 for the green, and 1 for the frontier.

To calculate with 9 intervals, instead of 11, the advantage of $f_{max} = 1.47$ goes more closer to the theoretical value $d_B(F) = 1.65$, because the calculation with a lower number of points is better in quantitative aspects, but worst in qualitative ones. From a practical point of view it

$\Delta\alpha$ interval number	Initial α of each interval $\Delta\alpha$	$N\alpha$ Number of boxes in each interval $\Delta\alpha$	Ln $N\alpha$
1	1.025	50	3.912
2	1.222	253	5.533
3	1.419	1450	7.279
4	1.616	2021	7.611
5	1.814	1023	6.930
6	2.011	638	6.458
7	2.208	486	6.186
8	2.405	406	6.006
9	2.603	307	5.727
10	2.800	192	5.257
11	2.997	55	4.007

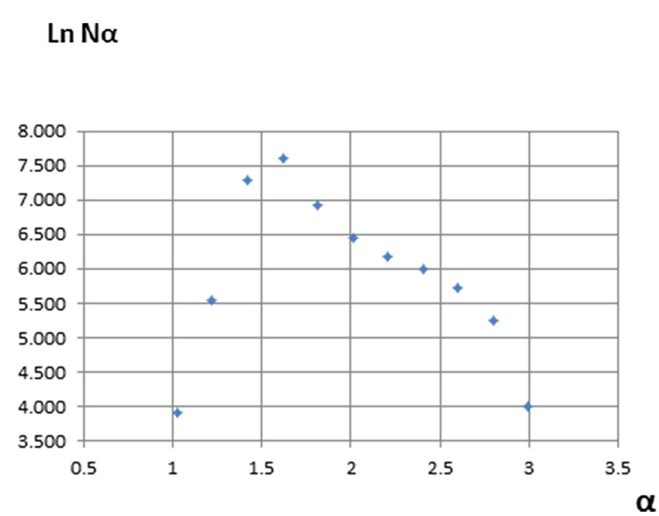

Fig. 6. Multifractal spectral values for 11 intervals.

Δα interval number	Initial α of each interval Δα	Nα Number of boxes in each interval Δα	Ln Nα
1	1.111	43	3.761
2	1.222	253	5.533
3	1.419	1450	7.279
4	1.616	2021	7.611
5	1.814	1023	6.930
6	2.011	638	6.458
7	2.208	486	6.186
8	2.405	406	6.006
9	2.603	307	5.727
10	2.800	192	5.257
11	2.997	55	4.007

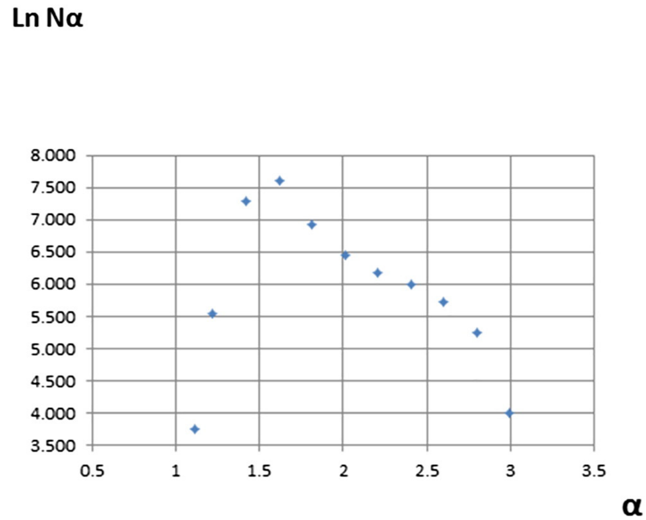

Fig. 7. Calibrated multifractal spectral values for 11 intervals.

is considered acceptable if $d_B(F)/f_{max} \le 1.33$. In this case $d_B(F)/f_{max} = 1.65/1.47 = 1.12$, which is really good.

Remarks

1. Each spectrum (red and green) has its own f_{max}. But there is a unique f_{max} for the complete spectrum, which has to be close to $d_B(F)$. In this case, the f_{max} close to $d_B(F)$ corresponds to the red spectrum, and confirms a mathematical property: if there are two objects with different fractal dimension, then the d_B (union of both objects, in this case red and green) $= d_B$(object of higher dimension, in this case the red).
2. As we have said, a multifractal spectrum $(\alpha, f(\alpha))$ has to be tangent, where $f' = 0$ to the horizontal $f(\alpha) = d_B(F) \cong f_{max}$, and also tangent to the bisector of the first quadrant $f(\alpha) = \alpha$ (as "$y = x$"). The obtained spectrum fulfills the two conditions.
3. In the studied system, the two multifractals correspond to two zones geographically separated. We call this structure "two-multifractal".
4. System stability. There are in the literature many examples where if the number of Δα intervals is changed, the spectrum changes qualitatively. In the studied system this problem does not occur, as can be seen in Figs. 11 and 12. This stability property of this system is rare and outstanding in an empirical situation of multifractal analysis.
5. Pre-multifractal fractal dimension. To confirm that the object is a true fractal it is necessary to confirm that the $d_B(F) = 1.65$ could be obtained (approximately) even in the case in which the boxes covering the possible fractal change in size and location, i.e. changing "L" and then N(L) in the expression $d_B = \text{Log } N(L)/\text{Log } (1/L)$ the results do not change.

The expression "$\text{Log } N(L) = d_B * \text{Log } (1/L)$" has to be independent of the value of "L", from a theoretical point of view. In an empirical context, the typical test is to represent "Log N(L)" vs. "Log (1/L)" for several "L". Then if the result is a straight line "$\text{Log } N(L) = d_B * \text{Log } (1/L)$" passing through the origin, the fractality can be assumed. In Fig. 13 we present the results, for different box sizes, which are in good agreement with the straight line from the origin to the farthest point (which is the best approximation to the theoretical limit $L \to 0$, or $N \to \infty$).

6. Frontier between red and green fractals (scattering of red fractal). As a result of the multifractal analysis, all the customer demand

Initial α of each interval Dα	Red fractal	Scattering of the red fractal	Green fractal
1.111	3.761		
1.222	5.533		
1.419	7.279		
1.616	7.611		
1.814	6.930		
2.011		6.458	
2.208			6.186
2.405			6.006
2.603			5.727
2.8			5.257
2.997			4.007

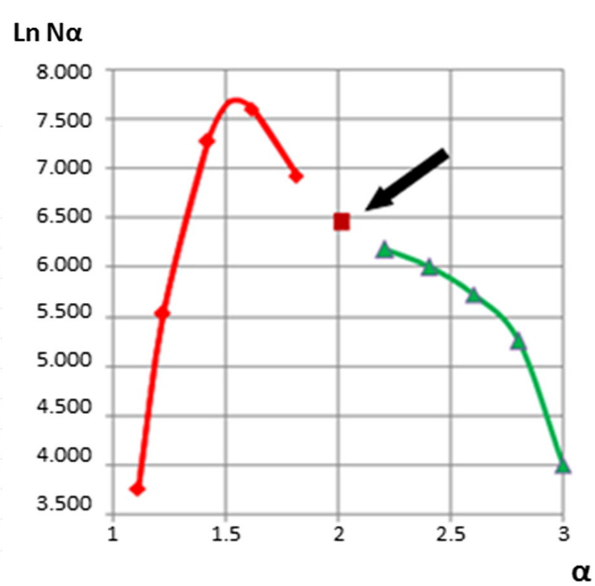

Fig. 8. Split multifractal spectrum for 11 intervals.

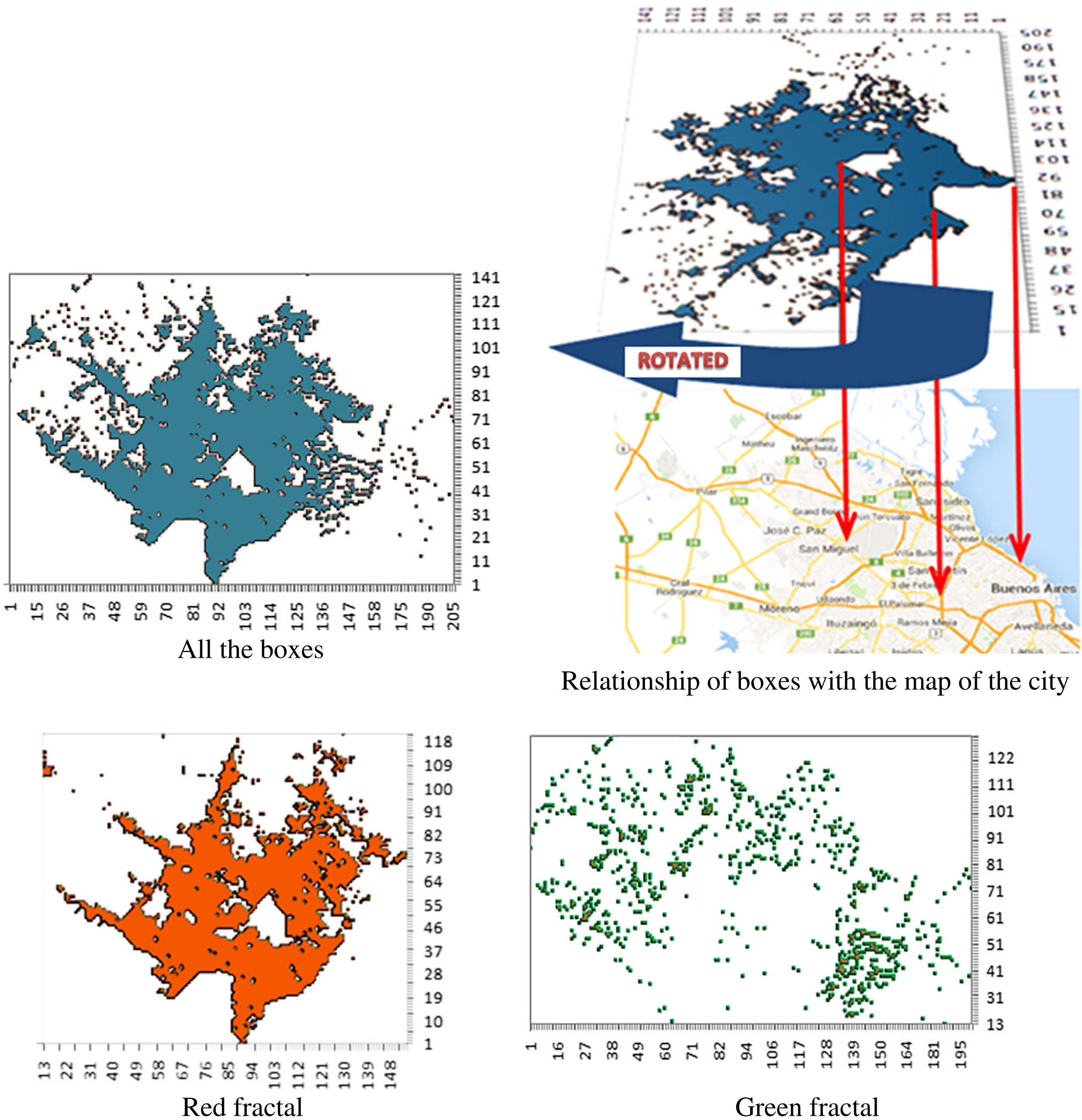

Fig. 9. Plan view of the customer area and its fractals.

was split into two zones, geographically separated, and shown in Fig. 9, the core red fractal and the peripheral green fractal. Between them there exists a frontier corresponding to a unique point of the (α, $f(\alpha)$), with α slightly greater than 2, which is at the same time an outer frontier for the red fractal (scattering at the right), and an inner frontier for the green fractal (scattering at the left). Fig. 14 shows the red fractal, plus the frontier points (black dots), and it can be seen that the frontier is a geographic frontier, surrounding the red zone of great demand represented by the heaviest boxes.

7. Sub-fractal frontier in detail. It has $N_\alpha = 638$ points, with α from 2.0108 to 2.2081. In this sub-fractal it is possible to obtain its multifractal spectrum as an independent problem. Because N_α is greater than 600, the unit will be 100, and then the interval [2.0108, 2.2081] is divided in 7 subintervals $\Delta\alpha$. The ratio of maximum and minimum $f(\alpha)$ in this interval is 1.07 which is approximately 1, i.e. $f(\alpha)$ is constant from a practical point of view in this interval, which means same dimension for subsets of different probability or different weight or measure.

Fig. 10 shows that the fractal dimension of this frontier fractal is 1.24. If the dimension were 1, and constant, it could be visualized as a line surrounding the red fractal, formed by an irregular polygonal of smooth curves or segments of different length. Since the dimension is different from 1, it is not a line, but because the dimension is constant, it maintains the “frontier” character, i.e. zones of the same dimension, but different measure, surrounding some region.

8. Scattering. Fig. 15 shows approximately 30 points that were discarded because they correspond to very light boxes, and we named them “Scattering at the right”. The red and green fractals are represented in this figure only for comparison purposes. These “30” point are scattered geographically.

Initial α of each interval Dα	Red fractal	Scattering of the red fractal	Green fractal	y=x
1.111	0.799			1.111
1.268	1.191			1.268
1.511	1.479			1.511
1.755	1.359			1.755
1.998		1.246		
2.242			1.190	
2.485			1.152	
2.729			1.041	
2.972			0.785	

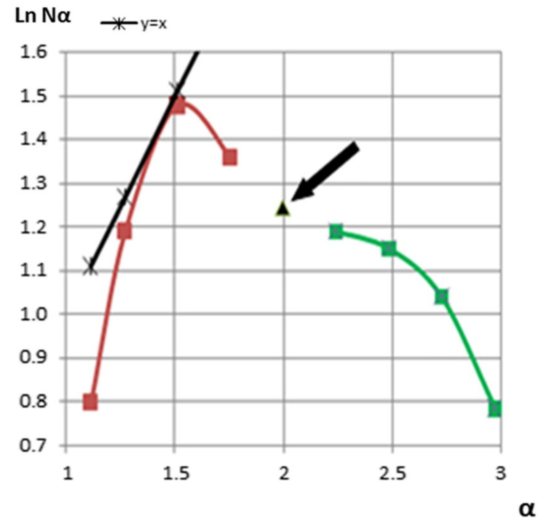

Fig. 10. Split multifractal spectrum for 9 intervals.

It is also possible to show the geographical situation of the 7 abnormally heavy points which we also discarded. Fig. 16 show that these points are not connected among themselves. Once identified, it is possible to perform other analyses of these customers: e.g. type of consumer, substation from where they are supplied electricity, etc.

Indices for the analysis and forecasting of the spatial growth of demand

The typical models for fractal growth, also in use to forecast the demographic growth of cities (Batty and Longley, 1994), called DLA (Diffusion Limited Aggregation) and DBM (Dielectric Breakdown Model) (Vicsek, 1992) are not necessarily adequate to forecast the electric demand, because it is necessary to know, at the same time, the spatial and the temporal growth of that demand, which could be different for different kinds of customers, and as we have seen, are not disordered and random, but is structured in the light of multifractal analysis.

That is the reason why we have developed some indices applying the results of the multifractal analysis, as a first step to the development of a more complete model in the future. The indices have to be applied to a definite period in time, by example, year, month, season, with the idea of comparing these indices periodically. Some of them are defined for the spectrum as a whole, and others for the red and/or green fractals, but can be generalized for multifractal distributions that can be different from the one we have analyzed. We present below ten indices, where the notation "r" o "g" means red or green spectrum.

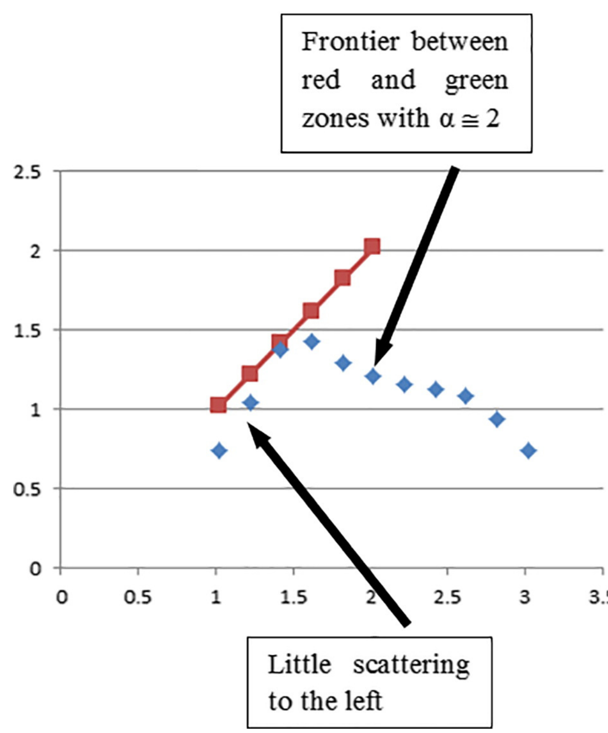

Fig. 11. For 11 intervals Δα, considering 7 initial points, but without 30 final points.

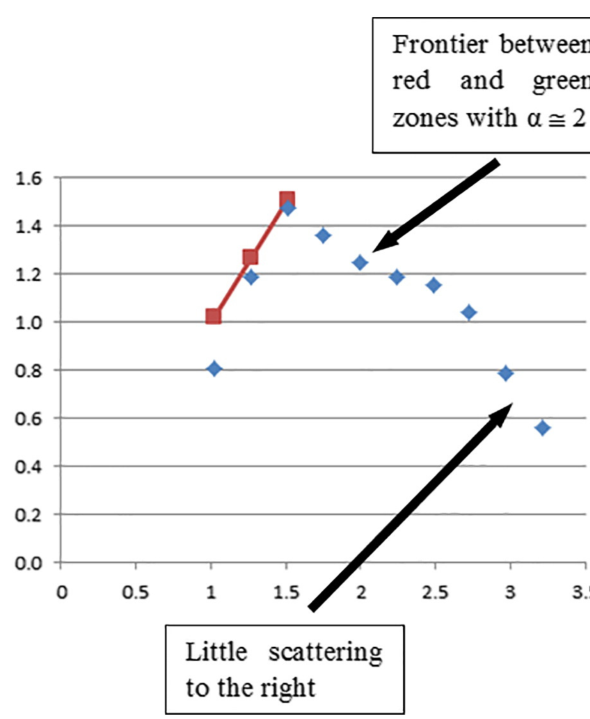

Fig. 12. For 10 intervals Δα, discarding α ≥ 3,5.

Box size	Box side	N Number of occupied boxes	log side	log N	log N/ log side
0,5x0,5km	1/208	6913	2.318	3.840	1.656
1x1km	1/104	2282	2.017	3.358	1.665
2x2km	1/52	776	1.716	2.890	1.684
4x4km	1/26	254	1.415	2.405	1.700

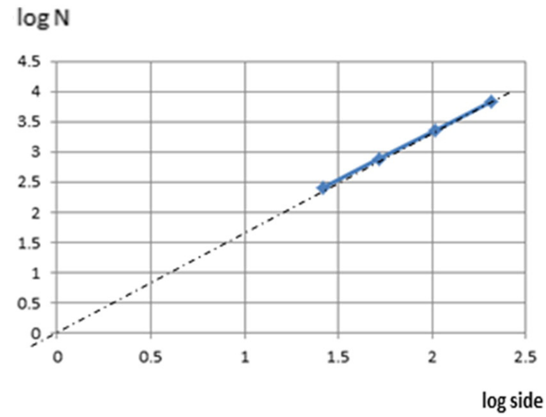

Fig. 13. Pre-multifractal fractal dimension.

Indices for the variation of demand, in the α axis

$$I_1^r = \alpha^r_{\max} - \alpha^r_{\min}$$

I_1 measures the increase or decrease of “high” demand (red fractal).
Applied to the green fractal, I_1^g measures the increase or decrease of “low” demand.

Indices for the variation of demand, in the f(α) axis

At the beginning, we consider only the maximum value of each subfractal of the spectra.

$$I_2^r = f^r_{\max}$$

Refining the idea, it could be possible to think of an absolute or relative integrated variation of the demand:

$$I^r_{3abs} = \int_{\alpha^r_{min}}^{\alpha^r_{max}} [f^r(\alpha)] \cdot d\alpha$$

$$I^r_{3rel} = \frac{1}{(\alpha^r_{max} - \alpha^r_{min})} \int_{\alpha^r_{min}}^{\alpha^r_{max}} [f^r(\alpha)] \cdot d\alpha$$

However, because of the split of the total α span into identical $\Delta\alpha$s, and with n^r the number of parts corresponding to the red fractal, we have:

$$I^r_{3rel} = \frac{1}{n^r} \sum_{k=1}^{n^r} f^r(k)$$

Similar expressions can be obtained for the green fractal.

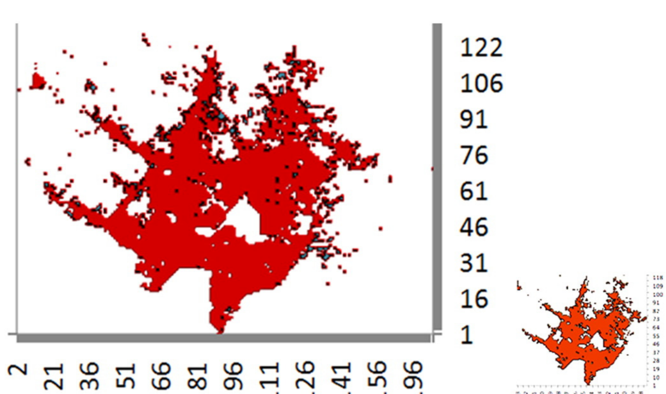

Fig. 14. Pre-multifractal fractal frontier between red and green fractals.

These indices represent other ways to measure the increase or decrease of “high” demand (red fractal) or the increase or decrease of “low” demand (green fractal).

Variation of the highest (or lowest) demand, integrated, absolute or relative

For the red fractal, the lowest α corresponds to the heaviest boxes, i.e. those with the highest demand.
But it may happen that $f^r(\alpha^r_{\min})$ varies without variation of $f^r_{\max}$, which means that there is a variation of the highest demand. Then, by integrating the red fractal only at the left:

$$I^r_{4abs} = \int_{\alpha^r_{min}}^{\alpha^r(f^r_{max})} [f^r(\alpha)] \cdot d\alpha$$

$$I^r_{4rel} = \frac{1}{[\alpha^r(f^r_{max}) - \alpha^r_{min}]} \int_{\alpha^r_{min}}^{\alpha^r(f^r_{max})} [f^r(\alpha)] \cdot d\alpha$$

Similarly, the variation of the lowest demand can be obtained by integrating the green fractal between $\alpha^g(f^g_{\max})$ y $\alpha^g_{\max}$.

Indices for the frontier points ($\alpha_{frontier}$, $f(\alpha_{frontier})$) between red and green spectra

If α_{frontier} is higher next year than the previous, it means that an important part of the customer universe has increased its energy demand. The following index can show this situation:

$$I_5 = \alpha_{frontier}$$

Nevertheless, if $f(\alpha_{\text{frontier}})$ goes up the next year, then the dimension of the frontier fractal goes up, i.e. the fractality of the frontier is increasing, which means that lower and higher demands are mixing together in a geographical sense. The following index can show this situation:

$$I_6 = f(\alpha_{frontier})$$

Spectral asymmetry

It can be seen in Fig. 10 that for the analyzed system the red spectrum is asymmetric. Then α^r $(f^r_{\max})$ is located closer to $\alpha^r_{\max}$ than to $\alpha^r_{\min}$. This spectral asymmetry can be evaluated in the following way:

$$I_7 = [\alpha^r(f^r_{\max}) - \alpha^r_{\min}] / [\alpha^r_{\max} - \alpha^r(f^r_{\max})]$$

This index shows the ratio of the demand, inside the red fractal, i.e. of the high demand, which is performed near its own maximum value (in the case of red fractal, the heavy boxes, $\alpha^r_{\min}$), vis a vis the demand close to its own minimum value (for the red fractal, the light boxes, $\alpha^r_{\max}$). In

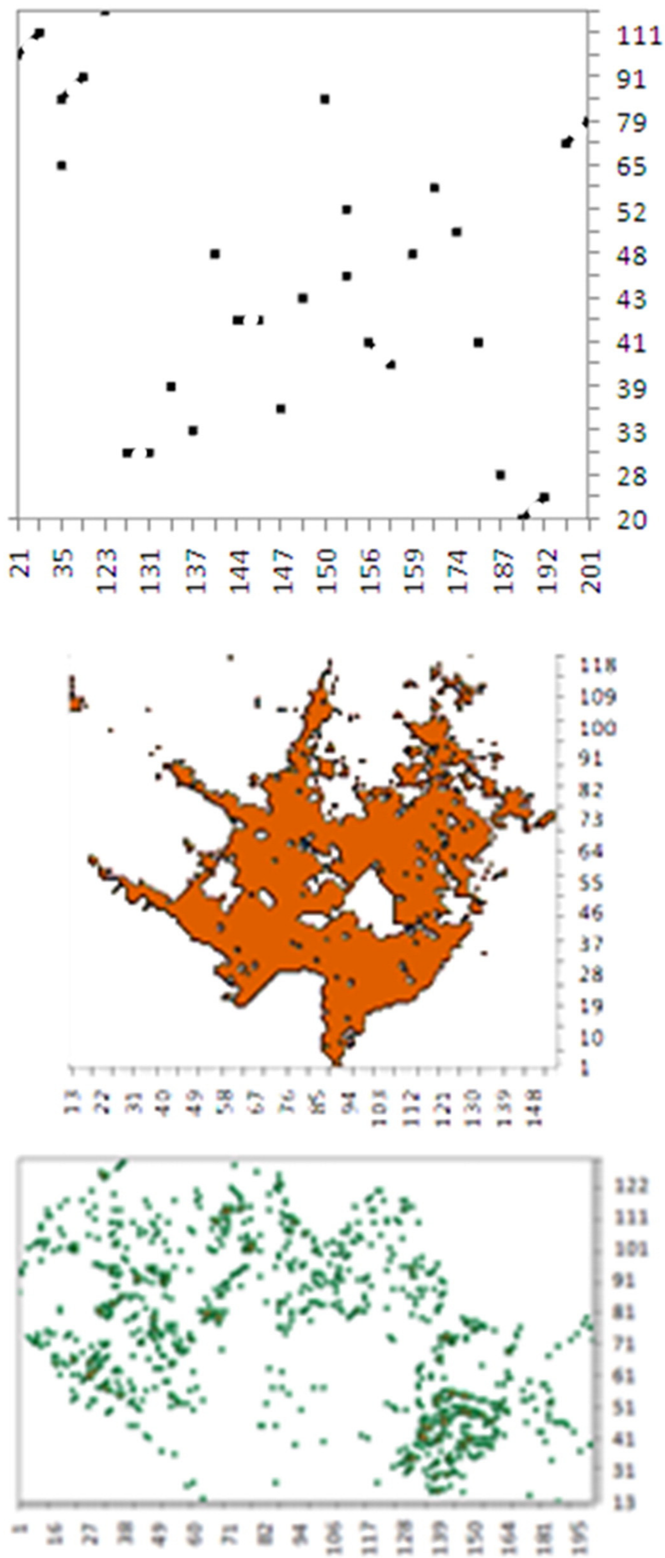

Fig. 15. Scattering at the right.

this case, the asymmetry is for the α coordinate. And for the asymmetry in the f (α) coordinate, we have:

$$I_8 = \left[f^r_{\max} - f^r\left(\propto^r_{\max}\right)\right] / f^r_{\max}$$

Lower values of I_8 show that customers with lower demand, inside the red fractal, demand energy in the same ratio as the majority of the

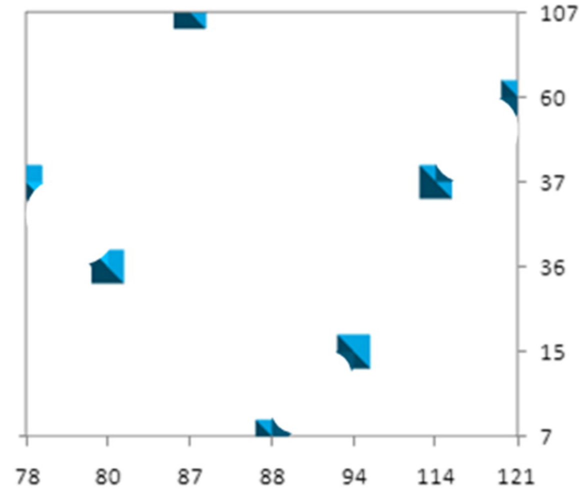

Fig. 16. Scattering at the left.

customers of the red fractal, which means that for these customers their f(α)s are not very different from $f^r(\alpha_{max})$.

Indices obtained by application of the thermodynamic algorithm and information theory

The theory of multifractality can be read from two points of view. Up to the moment we have related "α" to "Concentration" and "f (α)" to "Dimension". But another point of view, based in the as called "Thermodynamic Algorithm" relates "α" to "Internal Energy" and "f (α)" to "Entropy", as the analogues in statistical mechanics. Here it is important to consider the "notable point" ($\alpha_{entropic}$, $f(\alpha_{entropic})$) of the spectrum, which is where $f'(\alpha) = 1$ y $f(\alpha) = \alpha$. This point has two useful meanings for electricity demand:

- From a purely fractal point of view, the subfractal $F\alpha_{entropic}$ is the most self-similar of the spectrum, really the only self-similar one.
- By applying Information Theory, it is possible to assess that this subfractal contains all the information about the probability measure of each box. Its dimension $f(\alpha_{entropic})$, which is called "Information dimension" or "Entropic dimension" is the "best mean value" (considering arithmetic, geometric, logarithmic, etc. mean values) to synthesize in a single value the whole spectrum of multifractal dimensions. The following indices can show this situation:

$$I_9 = \alpha^r\left(f^r_{max}\right) - \alpha_{\text{entropico}}$$

$$I_{10} = f^r_{max} - f\left(\alpha_{\text{entropico}}\right) = f^r_{max} - \alpha_{\text{entropico}}$$

These indices are really significant because they evaluate the deviation of the maximum of the spectrum from its own mean value, because f^r_{max} typifies the absolute majority of customers who have a high energy consumption, given by α^r (f^r_{max}).

Conclusions

We have proposed a new point of view to forecast the spatial growth of the electricity demand. This new focus adds value to the traditional tools in use by utilities, but does not replace them. As a result of the applied method, the customer demand analyzed has been split into a "two-multifractal" (core urban zone with higher demand, surrounded by a suburban zone with lower demand), with a frontier between them, showing that the apparently random distribution of the demand has an internal structure only visible by using multifractal analysis.

The obtained spectra show properties (stability, constant dimensionality of the frontier, etc.) uncommon in the literature on fractals in an empirical context.

We have presented indices to compare the multifractal distributions in regular periods and to extrapolate the trends to the future.

The procedure could be improved from a geographic and demographic focus, by considering "urban models" (Willis, 2002) and "land use models", adjusted to the region where the utilities work. The final model must include impact demands, distributed generation, and the driving force behind the growth of the demand, perhaps using physical analogies based on the thermodynamic algorithm.

References

Batty M, Longley P. Fractal cities – a geometry of form and function. USA: Academic Press; 1994.

Czerkauer-Yamu C, Frankhauser P. A multi-scale (multi-fractal) approach for a systemic planning strategy from a regional to an architectural scale. Proc. REAL CORP 2010, Viena, Austria; 2010. Mayo.

Falconer K. Fractal geometry – mathematical foundations and applications. 2nd. ed. England: Wiley; 2003.

Frankhauser P. The fractal approach. A new tool for the spatial analysis of urban agglomerations. Population 1998;10(1):205–40.

Jonscher AK. Dielectric relaxation in solids. London: Chelsea Dielectrics Press; 1983.

Jonscher AK. All forms of relaxation take place in fractal time. IEEE Electr Insul Mag 1995; 11(2):30–3.

Kholladi M-K. Fractal structure of the urban objects. Int Arab J Inf Technol 2004;1(2). (Jul.).

Mandelbrot BB. The fractal geometry of nature. USA: W.H. Freeman and Co; 1977.

Piacquadio Losada MN. Los fractales y el árbol de Farey; 2011. unpublished book.

Piacquadio M, Rosen M. Multifractal spectrum of an experimental (video feedback) Farey tree. J Stat Phys May 2007;127(4):783–804.

Rosen M, Piacquadio M. Multifractal analysis of a road-to-crisis in a Faraday experiment (arXiv: 0804.3426v2); 2008.

Sharma KM, Sreedhar PN. A heuristic expert system for dynamic planning of electrical distribution systems. Congress CIDEL Argentina; 2002.

Tannier C, Pumain D. Fractals in urban geography: a theoretical outline and an empirical example. Eur J Geogr 2005. (document 307, http://cybergeo.revues.org/index3275.html, on line 20 Apr.).

Thibault S. "The morphology and growth of urban technical networks: a fractal approach", flux N° 19 (Jan.-Mar.); 1995.

Vicsek T. Fractal growth phenomena. 2nd. ed. Singapore: World Scientific; 1992.

Vieira Tahan CM, Pereyra Zamora FH. Redes neurais artificiais aplicadas na previsao espacial de carga eletrica em sistemas de distribucao. Buenos Aires, Argentina: Congress CIDEL; 2002.

Willis HL. Spatial electric load forecasting. 2nd. ed. New York: Marcel Dekker Inc.; 2002.